Electronic Distribution in the Metal-to-Ligand Charge Transfer (MLCT) Excited States of $[(4,4'\text{-}(X)_2bpy)(CO)_3Re^{I}(4,4'\text{-}bpy)Re^{I}(CO)_3(4,4'\text{-}(X)_2bpy)]^{2+}$ (X = H, CH_3). Application of Time-Resolved Infrared and Resonance Raman Spectroscopies

Kristin M. Omberg, Jon R. Schoonover,* and Thomas J. Meyer*

Department of Chemistry, CB#3290, University of North Carolina, Chapel Hill, North Carolina 27599-3290, and the Bioscience and Biotechnology Group (CST-4), Chemical Science and Technology Division, Mail Stop J586, Los Alamos National Laboratory, Los Alamos, New Mexico 87545

Received: August 1, 1997[⊗]

Ground- and excited-state resonance Raman and infrared spectra (354.7 nm excitation, in acetonitrile at 298 K) have been measured for $[(4,4'\text{-}(X)_2bpy)(CO)_3Re^{I}(4,4'\text{-}bpy)Re^{I}(CO)_3(4,4'\text{-}(X)_2bpy)]^{2+}$ (bpy is 2,2′-bipyridine; 4,4′-bpy is 4,4′-bipyridine; X = H, CH_3). The lowest lying excited states in these molecules are metal-to-ligand charge transfer (MLCT) in character. The spectra provide answers to two questions: Is the acceptor ligand for the excited electron 4,4′-bpy or $4,4'\text{-}(X)_2bpy$? Are there localized ($Re^{II}-Re^{I}$) or delocalized ($Re^{I.5}-Re^{I.5}$) sites in the mixed-valence excited states formed by MLCT excitation? Application of time-resolved resonance Raman (TR^3) spectroscopy demonstrates that 4,4′-bpy is the acceptor in the lowest lying MLCT excited state(s) of $[(dmb)(CO)_3Re(4,4'\text{-}bpy)Re(CO)_3(dmb)]^{2+}$* (dmb = $4,4'\text{-}(CH_3)_2bpy$) and that there is an equilibrium between 4,4′-bpy and bpy as acceptor in $[(bpy)(CO)_3Re(4,4'\text{-}bpy)Re(CO)_3(bpy)]^{2+}$*. For both complexes, the appearance of two sets of overlapping ν(CO) bands in the excited state by time-resolved infrared (TRIR) measurements is consistent with the localized description, $Re^{II}-Re^{I}$.

Introduction

Ligand-bridged, polypyridyl complexes of Re^{I}, Os^{II}, and Ru^{II} have proven useful in the study of photoinduced electron and energy transfer.[1] The electronic structures of these complexes are often complicated by low overall molecular symmetries, a high degree of spin−orbit coupling at the metal, and the existence of multiple π* acceptor levels on the polypyridyl ligands.[2] The energies of the lowest lying excited states are affected by the substituents on the polypyridyl ligands and the other ligands in the coordination sphere.[3] Often, states are sufficiently close in energy that more than one contributes to excited-state properties.

In the ligand-bridged Re^{I} complexes, $[(4,4'\text{-}(X)_2bpy)(CO)_3Re^{I}(4,4'\text{-}bpy)Re^{I}(CO)_3(4,4'\text{-}(X)_2bpy)]^{2+}$ (bpy is 2,2′-bipyridine; 4,4′-bpy is 4,4′-bipyridine; X = H, CH_3, NH_2, CO_2Et), there are low-lying π* acceptor levels on both 2,2′-bpy and the 4,4′-bpy bridge.[4] The relative energies of metal-to-ligand charge-transfer (MLCT) excited states and the associated excited-state electronic distributions are determined by the 2,2′-bpy substituents, −X. Earlier results based on transient absorption measurements suggested that when −X is electron-withdrawing $-CO_2Et$, the lowest MLCT state is localized on $4,4'\text{-}(CO_2Et)_2bpy$. With −X electron-donating $-CH_3$, the excited state is on the bridge. With X = H, the acceptor abilities of 2,2′-bpy and 4,4′-bpy are comparable and an equilibrium exists between bridge-based and terminal MLCT excited states.[4] Although reasonable, these conclusions were drawn from broad, featureless transient absorption difference spectra and are not without equivocation.

It was not possible in earlier studies to address a second issue relating to electronic structure, mixed-valence character across the ligand bridge. MLCT excitation to either the bridge or terminal bpy ligands creates a mixed-valency, and the resulting excited states could be localized or delocalized, as illustrated for the bridge-based excited state in example **1**,

$[(4,4'\text{-}(X)_2bpy)(CO)_3Re^{II}(4,4'\text{-}bpy^{\bullet-})Re^{I}(CO)_3(4,4'\text{-}(X)_2bpy)]^{2+}$*
1a (*localized*)

$[(4,4'\text{-}(X)_2bpy)(CO)_3Re^{I.5}(4,4'\text{-}bpy^{\bullet-})Re^{I.5}(CO)_3(4,4'\text{-}(X)_2bpy)]^{2+}$*
1b (*delocalized*)

With terminal bpy excitation, there is an additional ambiguity with regard to mixed-valence character at bpy, as illustrated in **2**,

$[(4,4'\text{-}(X)_2bpy^{\bullet-})(CO)_3Re^{II}(4,4'\text{-}bpy)Re^{I}(CO)_3(4,4'\text{-}(X)_2bpy)]^{2+}$*
2a (*localized*)

$[(4,4'\text{-}(X)_2bpy^{1/2\bullet-})(CO)_3Re^{I.5}(4,4'\text{-}bpy)Re^{I.5}(CO)_3(4,4'\text{-}(X)_2bpy^{1/2\bullet-})]^{2+}$*
2b (*delocalized*)

Isomers with spatial separation of the excited electron−hole pair, e.g. **2c**, are at higher energy,[4]

$[(4,4'\text{-}(X)_2bpy)(CO)_3Re^{II}(4,4'\text{-}bpy)Re^{I}(CO)_3(4,4'\text{-}(X)_2bpy^{\bullet-})]^{2+}$*
2c (*localized*)

We report here application of excited-state vibrational spectroscopy to both issues based on time-resolved resonance Raman (TR^3) and infrared (TRIR) measurements on $[(4,4'\text{-}(X)_2bpy)(CO)_3Re(4,4'\text{-}bpy)Re(CO)_3(4,4'\text{-}(X)_2bpy)]^{2+}$* (X = H, CH_3) and the models $[(4,4'\text{-}(X)_2bpy)(CO)_3Re(4\text{-}Etpy)]^{+}$* (X = H, CH_3; 4-Etpy is 4-ethylpyridine). The structures of the ligands are illustrated below.

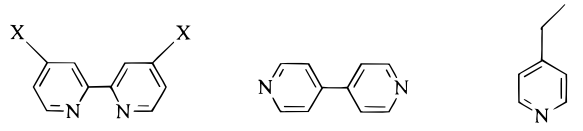

4,4'-$(X)_2$bpy (X = H, CH_3) 4,4'-bpy 4-Etpy

⊗ Abstract published in *Advance ACS Abstracts,* November 1, 1997.

S1089-5639(97)02522-X CCC: $14.00

Experimental Section

Materials. Acetonitrile was obtained from Burdick and Jackson and used without further purification. The salts $[(dmb)(CO)_3Re^I(4,4'\text{-bpy})Re^I(CO)_3(dmb)](PF_6)_2$ (dmb = 4,4′-$(CH_3)_2$-bpy), $[(bpy)(CO)_3Re^I(4,4'\text{-bpy})Re^I(CO)_3(bpy)](PF_6)_2$, $[(dmb)Re^I(CO)_3(4\text{-Etpy})](PF_6)$, and $[(bpy)Re^I(CO)_3(4\text{-Etpy})](PF_6)$ were prepared according to literature procedures.[4b,5]

Infrared Measurements. Infrared measurements utilized a BioRad FTS 60A/896 step-scan interferometer as previously described.[6] Data acquisition was gated between the laser pulse and 400 ns for TRIR spectra. Ground-state spectra are an average of 64 scans, and excited-state spectra an average of 32 scans.

Samples for TRIR Studies. All time-resolved infrared (TRIR) spectra were measured in acetonitrile. Sample concentrations were adjusted to give an IR absorbance of approximately 1.0 for the CO bands. The sample cell and sample solutions were deoxygenated by sparging with argon for 15 min; solutions were transferred to the cell under an inert atmosphere. Spectra were acquired in blocks of 16 scans to ensure sample integrity. No sample decomposition was observed during the acquisition periods.

Raman Measurements. Resonance Raman (RR) spectra were acquired by using continuous wave excitation at 406.7 nm from a Coherent Innova 90 Kr^+ laser. The scattered radiation was collected in a 135° backscattering geometry and passed into a Jobin Yvon U1000 double monochromator with an 1800 g/mm ruled grating. The signal was detected with an RCA 31034-C PMT and collected by using the Enhanced Prism software package from Instruments, S.A., Jobin Yvon. The final spectra were the average of 25 scans.

Time-resolved resonance Raman (TR^3) spectra were measured by using the third harmonic (354.7 nm) of a Quanta-Ray DCR-2A pulsed Nd:YAG laser both to create the excited state and as a source for the Raman scattering. The scattered radiation was collected in a 135° backscattering geometry into a SPEX 1877 Triplemate spectrometer equipped with an 1800 grooves/mm grating. The Raman signal was detected by a Princeton Instruments IRY-700G optical multichannel analyzer operating in the gated mode with a ST-110 OSMA detector-controller. Timing was controlled by a Princeton Instruments FG-100 pulse generator. The final spectra were the result of 9 min of total integration time. Laser power was between 3 and 5 mJ/pulse. Data collection and storage were controlled by an IBM AT with Princeton Instruments SMA software.

Samples for Raman Studies. All Raman spectra were acquired at ~4 mM in acetonitrile. Samples for time-resolved resonance Raman measurements were degassed by sparging with argon.

Results

Raman. In the resonance Raman (RR) spectrum of $[(dmb)(CO)_3Re(4,4'\text{-bpy})Re(CO)_3(dmb)]^{2+}$ (406.7 nm excitation, in acetonitrile at 298 K; dmb = 4,4′-$(CH_3)_2$bpy) 4,4′-bpy bands appear at 1029, 1070, 1233, 1301, and 1621 cm^{-1}.[7] Low-intensity dmb bands are also observed at 1495 and 1555 cm^{-1}.[8] In the TR^3 spectrum (354.7 nm excitation and scattering, in acetonitrile at 298 K), bands for 4,4′-bpy* (* denotes excited state)[7] appear at 1024, 1242, 1358, 1508, and 1625 cm^{-1}. (Analogous bands are observed in the RR spectrum of the 4,4′-bpy radical anion.[7a]) Ground-state dmb bands are also observed at 1034, 1214, 1282, 1495, 1556, and 1605 cm^{-1}.[8] The TR^3 spectrum between 1000 and 1700 cm^{-1} is shown in Figure 1A, and band energies and assignments for both spectra are listed in Table 1.

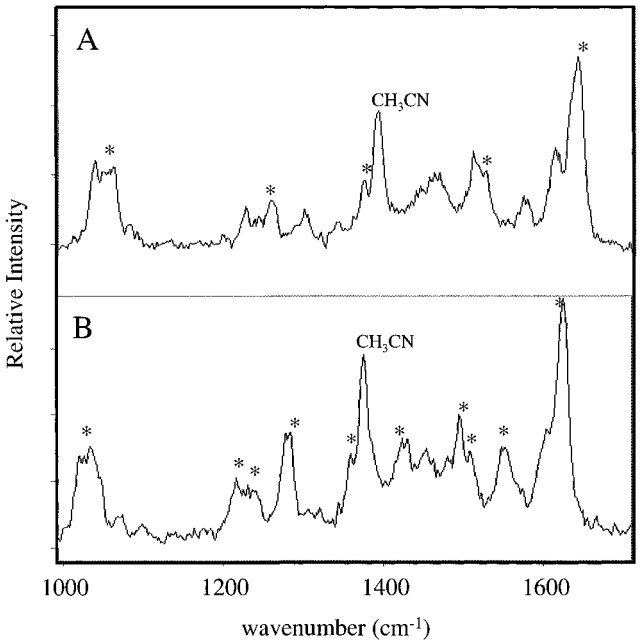

Figure 1. TR^3 spectra of $[(dmb)(CO)_3Re(4,4'\text{-bpy})Re(CO)_3(dmb)](PF_6)_2$ (A) and $[(bpy)(CO)_3Re(4,4'\text{-bpy})Re(CO)_3(bpy)](PF_6)_2$ (B) (354.7 nm excitation and scattering; dmb = 4,4′-$(CH_3)_2$bpy) in acetonitrile at 298 K). Excited-state bands are labeled with *.

TABLE 1: Ground- and Excited-State Raman Band Energies (cm^{-1}) and Assignments for $[(dmb)(CO)_3Re(4,4'\text{-bpy})Re(CO)_3(dmb)]^{2+}$ between 1000 and 1700 cm^{-1} at 298 K in CH_3CN (dmb = 4,4′-$(CH_3)_2$bpy)

ground state[a]		excited state[b]	
energy (cm^{-1})	assignment	energy (cm^{-1})	assignment
1029	4,4′-bpy	1024	4,4′-bpy*
		1034	dmb
1070	4,4′-bpy	1214	dmb
1233	4,4′-bpy	1242	4,4′-bpy*
1301	4,4′-bpy	1282	dmb
		1358	4,4′-bpy*
1495	dmb	1495	dmb
		1508	4,4′-bpy*
1555	dmb	1556	dmb
		1605	dmb
1621	4,4′-bpy	1625	4,4′-bpy*

[a] 406.7 nm excitation. Solvent bands appear at 1376 and 1445 cm^{-1} in both ground- and excited-state spectra. [b] 354.7 nm excitation and scattering. * denotes an excited-state band.

In the RR spectrum of $[(bpy)(CO)_3Re(4,4'\text{-bpy})Re(CO)_3(bpy)]^{2+}$, bands from both 2,2′-bpy[9] and 4,4′-bpy[7] appear (Table 2). In the TR^3 spectrum, bands from 4,4′-bpy*,[7] bpy, and bpy*[9] appear (Table 2). The TR^3 spectrum between 1000 and 1700 cm^{-1} is shown in Figure 1B.

Infrared Measurements. IR and TRIR spectra in the carbonyl region (1800−2200 cm^{-1}) for $[(dmb)(CO)_3Re(4,4'\text{-bpy})Re(CO)_3(dmb)]^{2+}$ and the model $[(dmb)Re(CO)_3(4\text{-Etpy})]^+$ (in acetonitrile at 298 K) are shown in Figure 2. For both complexes, bands appear in the ground-state spectrum originating from A and E modes in pseudo-C_{3v} symmetry (2035 and 1921 cm^{-1} for the dimer and 2034 and 1927 cm^{-1} for the monomer). In the excited-state spectrum of the monomer, bands appear at 2067, 2008, and 1964 cm^{-1}, shifted to higher energy relative to the ground-state bands. In the excited-state spectrum of the dimer, four bands appear, three shifted to higher energy, 2074, 2023, and 1981 cm^{-1}, and one to lower energy, 1910 cm^{-1}. Ground- and excited-state band energies are listed in Table 3.

TABLE 2: Ground- and Excited-State Raman Band Energies (cm^{-1}) and Assignments for $[(bpy)(CO)_3Re(4,4'\text{-}bpy)Re(CO)_3(bpy)]^{2+}$ between 1000 and 1700 cm^{-1} at 298 K in CH_3CN

ground state[a]		excited state[b]	
energy (cm^{-1})	assignment	energy (cm^{-1})	assignment[c]
1029	4,4′-bpy	1024	4,4′-bpy*
		1034	$\nu_{14'}$, bpy*
1072	4,4′-bpy	1214	$\nu_{11'}$, bpy*
1231	4,4′-bpy	1240	4,4′-bpy*
		1276	ν_{10}, bpy
1290	ν_{10}, bpy	1283	$\nu_{10'}$, bpy*
		1358	4,4′-bpy*
		1428	$\nu_{8'}$, bpy*
1444	ν_8, bpy	1454	ν_8, bpy
		1479	ν_7, bpy
1490	ν_7, bpy	1495	$\nu_{7'}$, bpy*
		1507	4,4′-bpy*
		1546	$\nu_{5'}$, bpy*
		1603	ν_5, bpy
1620	4,4′-bpy	1624	4,4′-bpy*

[a] 406.7 nm excitation. Solvent appears at 1376 cm^{-1} in both ground- and excited-state spectra. [b] 354.7 nm excitation and scattering. * denotes an excited-state band. [c] The bpy* assignments are from ref 9a.

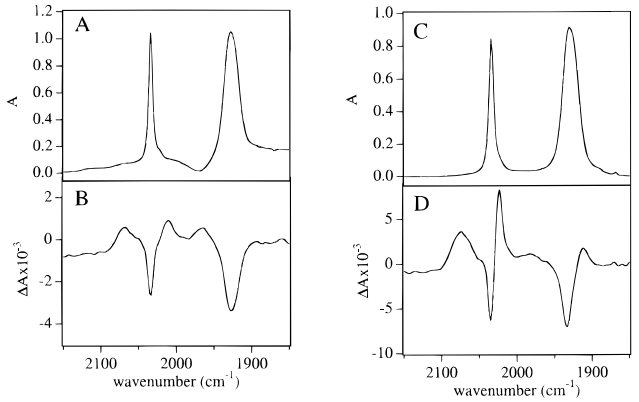

Figure 2. IR (A, C) and TRIR (B, D) spectra of $[(dmb)(CO)_3Re(4\text{-}Etpy)](PF_6)$ (A, B) and $[(dmb)(CO)_3Re(4,4'\text{-}bpy)Re(CO)_3(dmb)](PF_6)_2$ (C, D) (TRIR spectra 0−400 ns after laser flash excitation at 354.7 nm, ∼100 μJ/pulse; dmb = 4,4′-$(CH_3)_2$bpy) in acetonitrile at 298 K.

IR and TRIR spectra for $[(bpy)(CO)_3Re(4,4'\text{-}bpy)Re(CO)_3(bpy)]^{2+}$ and $[(bpy)Re(CO)_3(4\text{-}Etpy)]^{+}$ (in acetonitrile, at 298 K) are shown in Figure 3. Both exhibit two ground-state ν(CO) bands, at 2037 and 1933 cm^{-1} for the dimer and at 2035 and 1927 cm^{-1} for the monomer. In the excited-state spectrum of the monomer, three ν(CO) bands appear shifted to higher energy relative to the ground state, at 2074, 2010, and 1971 cm^{-1}. In the excited-state spectrum of the dimer, three bands appear at higher energy, at 2070, 2025, and 1977 cm^{-1}, and one at lower energy, at 1913 cm^{-1}. Band energies are listed in Table 3.

Discussion

The excited-state Raman and infrared spectra of $[(dmb)(CO)_3Re(4,4'\text{-}bpy)Re(CO)_3(dmb)]^{2+}$* and $[(bpy)(CO)_3Re(4,4'\text{-}bpy)Re(CO)_3(bpy)]^{2+}$* provide answers to the two questions posed in the Introduction: What is the acceptor ligand? What is the mixed-valence electronic distribution in the excited state?

Raman. In the RR spectrum of $[(dmb)(CO)_3Re^{I}(4,4'\text{-}bpy)Re^{I}(CO)_3(dmb)]^{2+}$ (406.7 nm excitation), a number of 4,4′-bpy bands are strongly resonantly enhanced,[7] while less strongly enhanced dmb bands appear at 1495 and 1555 cm^{-1}.[8] This pattern of enhancements is consistent with the absorption spectrum of the complex. In the low-energy region of this spectrum there is a broad, structured absorption centered at 340 nm which tails into the visible. It originates from overlapping $Re^{I} \rightarrow$ dmb, $Re^{I} \rightarrow$ 4,4′-bpy MLCT adsorptions, with the latter dominating absorptivity at lower energy.[4b]

TABLE 3: Ground- and Excited-State ν(CO) Infrared Band Energies in cm^{-1} for $[(4,4'\text{-}(X)_2bpy)(CO)_3Re(4,4'\text{-}bpy)Re(CO)_3(4,4'\text{-}(X)_2bpy)]^{2+}$ and $[(4,4'\text{-}(X)_2bpy)Re(CO)_3(4\text{-}Etpy)]^{+}$ at 298 K in Acetonitrile (dmb = 4,4′-$(CH_3)_2$bpy).[a] Solid Arrows Indicate Shifts to Higher Energy; Dashed Arrows Indicate Shifts to Lower Energy

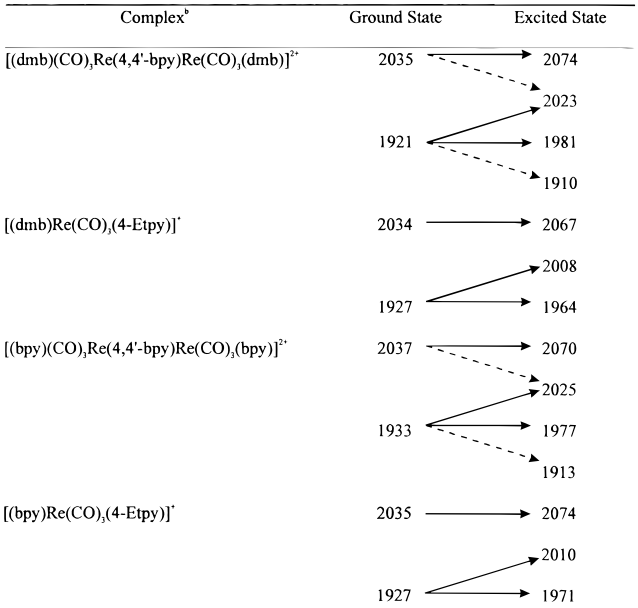

[a] 0−400 ns after laser flash excitation at 354.7 nm, ∼100 mJ/pulse. [b] As PF_6^- salts.

The TR^3 spectrum of $[(dmb)(CO)_3Re(4,4'\text{-}bpy)Re(CO)_3(dmb)]^{2+}$* was acquired with 354.7 nm excitation and scattering. This wavelength is on the high-energy side of $\pi \rightarrow \pi^*$ (dmb* or 4,4′-bpy*) absorptions of the MLCT excited states.[4b] Resonance enhancement is dominated by excited-state 4,4′-bpy bands, labeled as 4,4′-bpy* in Table 1.[7] Ground-state dmb bands at 1495 and 1555 cm^{-1} also appear[8] because the 354.7 nm excitation line is in near-resonance with a dmb $\pi \rightarrow \pi^*$ band at 318 nm and a Re $\rightarrow$ dmb band at 340 nm.[4b] There is no significant enhancement of excited-state dmb bands. These data are consistent with a lowest lying $Re^{II}(4,4'\text{-}bpy^{\bullet-})$-based MLCT excited state with no appreciable population of $Re^{II}(dmb^{\bullet-})$.

In the RR spectrum of $[(bpy)(CO)_3Re^{I}(4,4'\text{-}bpy)Re^{I}(CO)_3(bpy)]^{2+}$ (406.7 nm excitation) both 2,2′-bpy and 4,4′-bpy bands are enhanced.[7,9] In the TR^3 spectrum (354.7 nm excitation and scattering), bands for 4,4′-bpy*, bpy*,[9] and bpy all appear, the latter by $\pi \rightarrow \pi^*$ (bpy) and MLCT (bpy) enhancement as for the dmb dimer. The enhancement of *both* 4,4′-bpy* and 2,2′-bpy* bands is consistent with the earlier suggestion that there is an equilibrium between 4,4′-bpy- and 2,2′-bpy-based MLCT excited states,[4a] Scheme 1. In earlier studies,[4a] transient absorption measurements revealed that interconversion between isomers occurs on the <5 ns time scale, with k_2, $k_{-2} \gg k_1$, k_3 in Scheme 1. The oxidation state distribution in Scheme 1 is based on the TRIR results described in the next section.

Infrared. Two ν(CO) bands appear in the ground-state IR spectra of $[(dmb)(CO)_3Re^{I}(4,4'\text{-}bpy)Re^{I}(CO)_3(dmb)]^{2+}$ and $[(dmb)Re^{I}(CO)_3(4\text{-}Etpy)]^{+}$, consistent with pseudo-C_{3v} symmetry in both complexes. The fact that local pseudo-C_{3v} symmetry is maintained in the ligand-bridged complex is consistent with a small degree of $Re^{I}-Re^{I}$ electronic coupling and minor electronic perturbation across the 4,4′-bpy bridge.

SCHEME 1

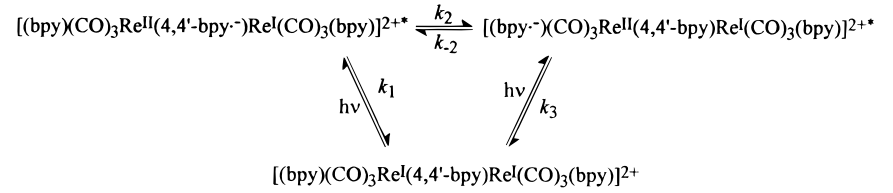

In the excited-state IR spectrum of [(dmb)Re(CO)$_3$(4-Etpy)]$^{+}$*, three ν(CO) bands appear shifted to higher energy relative to the ground state. The shifts to higher energy are consistent with partial oxidation at the metal and formation of the Re^{II}(dmb$^{\bullet-}$) MLCT excited state. The appearance of three bands rather than two is due to partial reduction at dmb, which lowers the effective local electronic symmetry to C_s.[2m,n,6,10] The E ν(CO) mode in the ground state is split into A′(CO) and A″(CO), which are well-separated and clearly resolvable in the excited state.

The pattern of three CO bands shifted to higher energy also appears in the excited-state spectrum of [(dmb)(CO)$_3$Re(4,4′-bpy)Re(CO)$_3$(dmb)]$^{2+}$* (Figure 2), but an additional band is also present shifted to lower energy. The intensity of the band at 2023 cm^{-1} is noticeably enhanced compared to the other three. A straightforward interpretation of the spectrum is that it consists of two sets of overlapping bands. There is one set of three bands, shifted to higher energy relative to the ground state, which appear at 2074, 2023, and 1981 cm^{-1}. A second set of two bands appears shifted to lower energy at 2023 and 1910 cm^{-1}. The three bands at higher energy are analogous to those observed in the excited-state spectrum of [(dmb)Re(CO)$_3$(4-Etpy)]$^{+}$*, consistent with a Re^{II}(polypyridyl$^{\bullet-}$) MLCT excited state. Based on the TR^3 spectrum, the acceptor ligand is 4,4′-bpy.

The appearance of two sets of bands indicates that the symmetry across the 4,4′-bpy bridge is lowered in the excited state and that there are two distinct Re sites. This is consistent with the excited-state electronic distribution in **1a**. Table 3 lists the energies of the ground- and excited-state bands and indicates the directions of the excited-state shifts. The A(CO) band at 2035 cm^{-1} in the ground state shifts to 2074 cm^{-1} in the MLCT excited state. The overlapping E(CO) bands at 1921 split and shift to A′(CO) at 1981 and A″(CO) at 2023 cm^{-1}, as indicated by the solid arrows in Table 3. These bands arise from the CO ligands at Re^{II} in [(dmb)(CO)$_3$Re^{II}(4,4′-bpy$^{\bullet-}$)*. They are analogous to those observed in the MLCT excited-state spectrum of [(dmb)Re(CO)$_3$(4-Etpy)]$^{+}$*. At the unexcited Re^{I}, −(4,4′-bpy$^{\bullet-}$)Re^{I}(CO)$_3$(dmb)]$^{+}$, E(CO) shifts 11 cm^{-1} to *lower* energy, to 1910 cm^{-1}, as indicated by the dashed arrow in Table 3. A(CO) appears to shift ∼12 cm^{-1} to lower energy, where it overlaps with the A″(CO) 2023 cm^{-1} band of Re^{II}(4,4′-bpy). The accidental overlap explains the unusually high intensity of this band.

The shifts to lower energy are due to localization of the excited electron on the 4,4′-bpy bridge. The partly reduced ligand donates electron density to Re^{I}. This increases Re^{I}−CO backbonding, decreases the CO bond order, and decreases the energy of ν(CO). A related effect has been observed in the TRIR spectrum of [(bpy)$_2$Ru^{II}ABRe^{I}(CO)$_3$Cl]$^{2+}$* (AB = 2,2′:3′2″:6″,2‴-quaterpyridine) in which the lowest MLCT excited state is on the bridge, [(bpy)$_2$Ru^{III}(AB$^{\bullet-}$)Re^{I}(CO)$_3$Cl]$^{2+}$*.[1b,6,11] As shown in Figure 4A, it is possible to construct the portion of the ν(CO) spectrum assigned to −(4,4′-bpy$^{\bullet-}$)Re^{I}(CO)$_3$-(dmb)]$^{+}$ by subtracting 1.6 × (monomer TRIR spectrum) from the TRIR spectrum of the dimer, both shown in Figure 2.

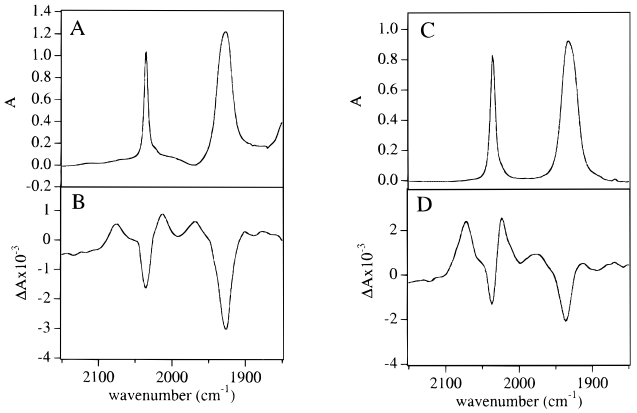

Figure 3. IR (A, C) and TRIR (B, D) spectra of [(bpy)(CO)$_3$Re(4-Etpy)](PF$_6$) (A, B) and [(bpy)(CO)$_3$Re(4,4′-bpy)Re(CO)$_3$(bpy)](PF$_6$)$_2$ (C, D) (TRIR spectra 0−400 ns after laser flash excitation at 354.7 nm, ∼100 μJ/pulse) in acetonitrile at 298 K.

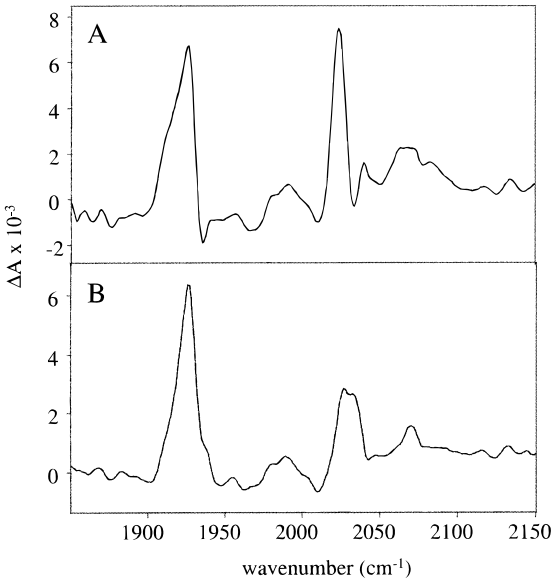

Figure 4. (A) Spectrum of −(4,4′-bpy$^{\bullet-}$)Re^{I}(CO)$_3$(dmb)]$^{+}$ in the excited state of [(dmb)(CO)$_3$Re^{II}(4,4′-bpy$^{\bullet-}$)Re^{I}(CO)$_3$(dmb)]$^{2+}$* (dmb = 4,4′-(CH$_3$)$_2$bpy) calculated by subtracting 1.6 × (spectrum B in Figure 2) from spectrum D in Figure 2. (B) Spectrum of −(4,4′-bpy$^{\bullet-}$)-Re^{I}(CO)$_3$(bpy)]$^{+}$ in the excited state of [(bpy)(CO)$_3$Re^{II}(4,4′-bpy$^{\bullet-}$)-Re^{I}(CO)$_3$(bpy)]$^{2+}$* calculated by subtracting 2.3 × (spectrum B in Figure 3) from spectrum D in Figure 3.

The magnitudes of the ν(CO) shifts at Re^{II} in the excited state of [(dmb)(CO)$_3$Re(4,4′-bpy)Re(CO)$_3$(dmb)]$^{2+}$* (+39, +102, +60 cm^{-1}) are greater than those in the monomer, [(dmb)Re-(CO)$_3$(4-Etpy)]$^{+}$* (+33, +81, +37 cm^{-1}). This is consistent with a greater degree of charge transfer to 4,4′-bpy compared to dmb as the acceptor ligand. This is a natural consequence of the single Re−N bond to 4,4′-bpy compared to the two Re−N bonds to a bidentate bpy or dmb acceptor. Re−N mixing is dominated by dπ(Re)−p(N) overlap. There are two overlaps for the bidentate ligands and a single overlap for 4,4′-bpy. A similar effect has been observed by Turner, George, and co-

workers in $[Re(4,4'\text{-bpy})_2(CO)_3Cl]^*$, where the excited electron is on a single 4,4′-bpy ligand and the excited state ν(CO) shifts are +38, +56, and +66 cm^{-1}.[12]

Data for $[(bpy)(CO)_3Re(4,4'\text{-bpy})Re(CO)_3(bpy)]^{2+*}$ and $[(bpy)Re(CO)_3(4\text{-Etpy})]^{+*}$ are also consistent with an MLCT excited state.[2m,n,6,10] In the excited-state spectrum of $[(bpy)(CO)_3Re(4,4'\text{-bpy})Re(CO)_3(bpy)]^{2+}$, four ν(CO) bands appear with the same overall pattern as the dmb dimer with only slight shifts in band energies between them. As for the dmb dimer, this spectrum can be interpreted as arising from two overlapping sets of bands: three at higher energy for Re^{II} and two at lower energy for Re^{I}. The spectrum at Re^{I} calculated by subtracting 2.3 × (monomer TRIR spectrum) from the dimer TRIR spectrum (in Figure 3) is shown in Figure 4B.

From the excited-state resonance Raman results, excitation of $[(bpy)(CO)_3Re^{I}(4,4'\text{-bpy})Re^{I}(CO)_3(bpy)]^{2+}$ gives both $[(bpy^{\bullet-})(CO)_3Re^{II}(4,4'\text{-bpy})Re^{I}(CO)_3(bpy)]^{2+*}$ and $[(bpy)(CO)_3Re^{II}(4,4'\text{-bpy}^{\bullet-})Re^{I}(CO)_3(bpy)]^{2+*}$, and both must contribute to the TRIR spectrum. The observed spectrum is the convolution of separate ν(CO) bands from $[(bpy^{\bullet-})(CO)_3Re^{II}(4,4'\text{-bpy})-]^{+*}$ and $[(bpy)(CO)_3Re^{II}(4,4'\text{-bpy}^{\bullet-})-]^{+*}$ at higher energy and $-(4,4'\text{-bpy}^{\bullet-})Re^{I}(CO)_3(bpy)]^{+}$ and $-(4,4'\text{-bpy})Re^{I}(CO)_3(bpy)]^{+}$ at lower energy. It is not possible to deconvolute separate sets of ν(CO) bands for $[(bpy^{\bullet-})(CO)_3Re^{II}(4,4'\text{-bpy})-]^{+*}$ and $[(bpy)(CO)_3Re^{II}(4,4'\text{-bpy}^{\bullet-})-]^{+*}$. The bandwidths are large (~30 cm^{-1}) and the energy difference must be too small to discern separate bands for these electronically closely related fragments.

The $-(4,4'\text{-bpy})Re^{I}(CO)_3(bpy)]^{+}$ fragment is not expected to contribute to the low-energy TRIR spectrum. With 2,2′-bpy as the acceptor ligand in $[(bpy^{\bullet-})(CO)_3Re^{II}(4,4'\text{-bpy})Re^{I}(CO)_3(bpy)]^{2+*}$, there is minimal perturbation at Re^{I}. The TRIR spectrum is a difference spectrum, and only features that undergo a change in energy or intensity are observed. The electronic difference between the ground and excited states is minimal for this fragment, and these bands apparently undergo no significant change upon excitation.

There is negative evidence for $-(4,4'\text{-bpy})Re^{I}(CO)_3(bpy)]^{+}$ in the excited-state spectrum. The intensities of the bands at 2025 and 1913 cm^{-1} are decreased relative to the analogous bands in the excited-state spectrum of $[(dmb)(CO)_3Re(4,4'\text{-bpy})Re(CO)_3(dmb)]^{2+*}$. This is consistent with the equilibrium in Scheme 1 and partial population of the 4,4′-bpy-based excited state.

The difference in electronic distribution between the MLCT excited states of $[(dmb)(CO)_3Re^{I}(4,4'\text{-bpy})Re^{I}(CO)_3(dmb)]^{2+}$ and $[(bpy)(CO)_3Re^{I}(4,4'\text{-bpy})Re^{I}(CO)_3(bpy)]^{2+}$ arises from substituent effects. With −H as the substituent, the energy of the bpy-based MLCT state is comparable to the energy of the 4,4′-bpy-based state (~2.12 eV for both, from emission measurements).[4] With electron-donating $-CH_3$ as the substituent in the dmb complex, the energy of the π^* acceptor level is increased, raising the energy of the dmb-based MLCT state sufficiently that this state is not appreciably populated at room temperature.[4b] This is a subtle example of using ligand "tuning" to modify MLCT excited-state structure.

Conclusions

On the basis of excited-state resonance Raman and IR measurements, 4,4′-bpy is the acceptor ligand in $[(dmb)(CO)_3Re(4,4'\text{-bpy}^{\bullet-})Re(CO)_3(dmb)]^{2+*}$. In $[(bpy)(CO)_3Re(4,4'\text{-bpy})Re(CO)_3(bpy)]^{2+*}$, there is an equilibrium between 4,4′-bpy and 2,2′-bpy as acceptors. Excited-state infrared spectra are consistent with localized valences and the mixed-valence electronic distribution $Re^{II}-Re^{I}$ in **1a** and **2a** in the Introduction. The delocalized structures **1b** and **2b** can be ruled out. This is an important example of the value of application of both TR[3] and TRIR spectroscopies to a complex system. In this case, time-resolved resonance Raman was the key to identifying the acceptor ligand and the time-resolved infrared, mixed-valence electronic distribution.

Acknowledgment. This work was performed in part at Los Alamos National Laboratory under the auspices of the U.S. Department of Energy and was supported by Laboratory Directed Research and Development Project No. 95101 to J.R.S. Work at the University of North Carolina was supported by the U.S. Department of Energy under Grant DE-FG02-96ER to T.J.M.

References and Notes

(1) (a) Balzani, V.; Juris, A.; Venturi, M.; Campagna, S.; Serroni, S. *Chem. Rev.* **1996**, *96*, 759. (b) Lu, H.; Petrov, V.; Hupp, J. T. *Chem. Phys. Lett.* **1995**, *235*, 521. (c) Bardwell, D. A.; Barigelletti, F.; Cleary, R. L.; Flamigni, L.; Guardegli, M.; Jeffery, J. C.; Ward, M. D. *Inorg. Chem.* **1995**, *34*, 2438. (d) Petrov, V.; Hupp, J. T. *J. Am. Chem. Soc.* **1994**, *116*, 2171. (e) Schoonover, J. R.; Gordon, K. C.; Argazzi, R.; Bignozzi, C. A.; Dyer, R. B.; Meyer, T. J. *J. Am. Chem. Soc.* **1993**, *115*, 10996. (f) Kalyansundaram, K. *Chemistry of Polypyridine and Porphyrin Complexes*; Academic Press: London, 1992. (g) Balzani, V.; Scandola, F. *Supramolecular Photochemistry*; Horwoord: Chichester, U.K., 1991. (h) Mikkelson, K. V.; Ratner, M. A. *J. Phys. Chem.* **1989**, *93*, 1759. (i) Balzani, V.; Barigelletti, F.; Campagna, S.; Belser, P.; von Zelewsky, A. *Coord. Chem. Rev.* **1988**, *84*, 85. (j) Ruminski, R. R.; Cockroft, T.; Shoup, M. *Inorg. Chem.* **1988**, *27*, 4026. (k) Murphy, W. R.; Brewer, K. T.; Petersen, J. D. *Inorg. Chem.* **1987**, *26*, 3376. (l) Brunschwig, B. S.; Ehrenson, S.; Sutin, N. *J. Phys. Chem.* **1986**, *90*, 3657. (m) Schanze, K. S.; Neyhart, G. A.; Meyer, T. J. *J. Phys. Chem.* **1986**, *90*, 2182. (n) Kambara, T.; Hendrickson, D. N.; Sorai, M.; Oh, S. M. *J. Chem. Phys.* **1986**, *85*, 2895. (o) Oh, S.; Hendrickson, D. N.; Hassett, K. L.; Davis, R. E. *J. Am. Chem. Soc.* **1985**, *107*, 8009. (p) Petersen, J. D.; Murphy, W. R.; Sahai, R.; Brewer, K. T.; Ruminski, R. R. *Coord. Chem. Rev.* **1985**, *64*, 261. (q) Creutz, C. *Prog. Inorg. Chem.* **1983**, *30*, 1. (r) Nishizawa, M.; Ford, P. C. *Inorg. Chem.* **1981**, *20*, 2016. (s) Creutz, C.; Taube, H. *J. Am. Chem. Soc.* **1969**, *91*, 3988. (t) Hush, N. S. *Prog. Inorg. Chem.* **1967**, *8*, 391.

(2) (a) Sacksteder, L. A.; Lee, M.; Demas, J. N. *J. Am. Chem. Soc.* **1993**, *115*, 18. (b) Indelli, M. T.; Binozzi, C. A.; Marconi, A.; Scandola, F. *J. Am. Chem. Soc.* **1988**, *110*, 7381. (c) Ferguson, J.; Krausz, E. *J. Lumin.* **1987**, *36*, 129. (d) Meyer, T. J. *Pure Appl. Chem.* **1986**, *58*, 1193. (e) Ferguson, J.; Herren, F.; Krausz, E.; Vrbancich, J. *Coord. Chem. Rev.* **1985**, *64*, 21. (f) Crosby, G. A.; Highland, R. G.; Truesdell, K. A. *Coord. Chem. Rev.* **1985**, *64*, 41. (g) DeArmond, M. K.; Hanck, K. W.; Wertz, D. W. *Coord. Chem. Rev.* **1985**, *64*, 65. (h) Caspar, J. V.; Sullivan, B. P.; Meyer, T. J. *Inorg. Chem.* **1984**, *23*, 2104. (i) Ohsawa, Y.; Whangbo, M.-H.; Hanck, K. W.; DeArmond, M. K. *J. Am. Chem. Soc.* **1983**, *105*, 3032. (j) Kober, E. M.; Meyer, T. J. *Inorg. Chem.* **1983**, *22*, 1614. (k) Ferguson, J.; Krausz, E. R. *Chem. Phys. Lett.* **1982**, *93*, 21. (l) Hager, G. D.; Crosby, G. A. *J. Am. Chem. Soc.* **1975**, *97*, 7031. (m) Hager, G. D.; Watts, R. J.; Crosby, G. A. *J. Am. Chem. Soc.* **1975**, *97*, 7037. (n) Wrighton, M. S.; Morse, D. L. *Organomet. Chem.* **1975**, *97*, 405. (o) Morse, D. L.; Wrighton, M. S. *J. Am. Chem. Soc.* **1974**, *96*, 261.

(3) (a) Anderson, P. A.; Deacon, G. B.; Haarman, K. H.; Keene, F. R.; Meyer, T. J.; Reitsma, D. A.; Skelton, B. W.; Strouse, G. F.; Thomas, N. C.; Treadway, J. A.; White, A. H. *Inorg. Chem.* **1995**, *34*, 6145. (b) Anderson, P. A.; Strouse, G. F.; Treadway, J. A.; Keene, F. R.; Meyer, T. J. *Inorg. Chem.* **1994**, *33*, 3863. (c) Worl, L. A.; Duesing, R.; Chen, P.; Ciana, L. D.; Meyer, T. J. *J. Chem. Soc., Dalton Trans.* **1991**, 849. (d) Denti, G.; Sabatino, L.; DeRosa, G.; Bartolotta, A.; DiMarco, G.; Ricevuto, V.; Campagna, S. *Inorg. Chem.* **1989**, *28*, 2755. (e) Denti, G.; Sabatino, L.; DeRosa, G.; Bartolotta, A.; DiMarco, G.; Ricevuto, V.; Campagna, S. *Inorg. Chem.* **1989**, *28*, 2755. (f) Barqawi, K. R.; Llobet, A.; Meyer, T. J. *J. Am. Chem. Soc.* **1988**, *110*, 7751. (g) Kober, E. M.; Marshall, J. L.; Dressick, W. J.; Sullivan, B. P.; Caspar, J. V.; Meyer, T. J. *Inorg. Chem.* **1985**, *24*, 2755. (h) Caspar, J. V.; Meyer, T. J. *Inorg. Chem.* **1983**, *22*, 2444. (i) Kober, E. M.; Meyer, T. J. *Inorg. Chem.* **1982**, *21*, 3967. (j) Caspar, J. V.; Kober, E. M.; Sullivan, B. P.; Meyer, T. J. *J. Am. Chem. Soc.* **1982**, *104*, 630.

(4) (a) Tapolsky, G.; Duesing, R.; Meyer, T. J. *J. Phys. Chem.* **1991**, *95*, 1105. (b) Tapolsky, G.; Duesing, R.; Meyer, T. J. *Inorg. Chem.* **1990**, *29*, 2285.

(5) (a) Tapolsky, G.; Duesing, R.; Meyer, T. J. *J. Phys. Chem.* **1989**, *93*, 3885. (b) Chen, P. Y.; Duesing, R.; Tapolsky, G.; Meyer, T. J. *J. Am. Chem. Soc.* **1989**, *111*, 8503.

(6) Schoonover, J. R.; Strouse, G. F.; Omberg, K. M.; Dyer, R. B. *Comments Inorg. Chem.* **1996**, *3*, 165.

(7) (a) Ould-Moussa, L.; Poizat, O.; Castellà-Ventura, M.; Buntinx, G.; Kassab, E. *J. Phys. Chem.* **1996**, *100*, 2072. (b) McNicholl, R.-A.; McGarvey, J. J.; Al-Obaidi, A. H. R.; Bell, S. E. J.; Jayaweera, P. M.; Coates, C. G. *J. Phys. Chem.* **1995**, *99*, 12268. (c) Poizat, O.; Buntinx, G.; Ventura, M.; Lautié, M. F. *J. Phys. Chem.* **1991**, *95*, 1245. (d) Barker, D. J.; Cooney, R. P.; Summers, L. A. *J. Raman Spectrosc.* **1987**, *18*, 443.

(8) Strouse, G. F.; Anderson, P. A.; Schoonover, J. R.; Meyer, T. J.; Keene, R. F. *Inorg. Chem.* **1992**, *31*, 3004.

(9) (a) Strommen, D. P.; Mallick, P. K.; Danzer, G. D.; Lumpkin, R. S.; Kincaid, J. R. *J. Phys. Chem.* **1990**, *94*, 1357. (b) Mallick, P. K.; Danzer, G. D.; Strommen, D. P.; Kincaid, J. R. *J. Phys. Chem.* **1988**, *92*, 5628. (c) Bradley, P. G.; Kress, N.; Hornberger, B. A.; Dallinger, R. F.; Woodruff, W. H. *J. Am. Chem. Soc.* **1981**, *103*, 7441. (d) Dallinger, R. F.; Woodruff, W. H. *J. Am. Chem. Soc.* **1979**, *101*, 4391.

(10) (a) Schoonover, J. R.; Bates, W. D.; Meyer, T. J. *Inorg. Chem.* **1996**, *35*, 273. (b) Turner, J. J.; George, M. W.; Johnson, F. P. A.; Westwell, J. R. *Coord. Chem. Rev.* **1993**, *125*, 101. (c) Glyn, P.; George, M. W.; Hodges, P. M.; Turner, J. J. *J. Chem. Soc., Chem. Commun.* **1989**, 165.

(11) Ward, M. D. *J. Chem. Soc., Dalton Trans.* **1993**, 1321.

(12) Gamelin, D. R.; George, M. W.; Glyn, P.; Grevels, F.-W.; Johnson, F. P. A.; Klotzbücher, W.; Morrison, S. L.; Russell, G.; Schaffner, K.; Turner, J. J. *Inorg. Chem.* **1994**, *33*, 3246.